



Shimoni Michal; Borghys Dirk & Acheroy Marc



Schroder Reinhard; Martin Chiari &
Helmut Suess



HySAR GOAL

The main objective of this research is to resolve the classification ambiguity of several man-made objects in urban and industrial scenes using fused polarimetric SAR, InSAR and hyperspectral data.

Main assumption

While the polarimetric SAR measurements are sensitive to the surface geometry and the dielectric constant of the illuminated surface, hyperspectral data provide information related to the biochemical origin and environment of the observed area.

Target Features

Residences, industrial buildings, nuclear power plants, airports and roads in rural-urban and industrial scenes

CONTENTS

- * Research area
- * E-SAR and E-SAR in HySAR
- * Comparison of characteristics between HyMap and E-SAR
- * Image processing methodologies:
Hyperspectral, PolSAR and Fusion

- HYMAP** * Object detection based on logistic regression (LR)
- * Classification detection based on (LR)
- * Discrimination of roof materials
- E-SAR** * Detection of dominant scatter point
- * Classification of man-made structure using the Pauli decomposition
- * Combination of SAR and Hyperspectral results

- * Gundrremingen power plant
- * Nuclear power plant structure classification using HyMAP data
- * Textural filter – SAR / Xhh
- * Classification of power plant structure based on Pauli decomposition
- * Pixel based fusion of multi channel SAR data

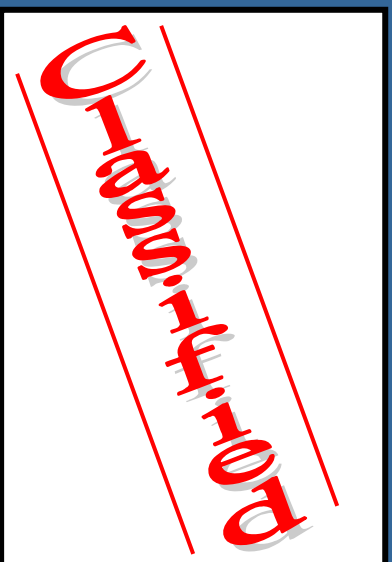
- * Conclusion and future research

RESEARCH AREAS

BruHyp Workshop, 7 October 2005, Bruges, Belgium



Gundramin



Cham-Hof

Penzlin



Oberpfaffenhohe

E-SAR

Operator

DLR, on DO-228

Frequency Range

X (9,6 GHz) L (1,3 GHz)

C (5,3 GHz) P (450 MHz)

S (3,3 GHz)

Polarization

The polarization of the radar signal is selectable:

horizontal and vertical

L-band operates in full polarisation (HH, VV, HV, VH)

Methods of Measurement

SAR-Interferometry

SAR-Polarimetry

Range Resolution

2,3 m (high resolution)

4,5 m (medium resolution)

Resolution (Azimuth)

0,6 m (1 look), 2 m (3 looks)

> 3 m (from 6 looks)

Swath Width on Ground

3 km (narrow swath)

5 km (wide swath)



E-SAR in HySAR

Frequency Range

X (9,6 GHz) L (1,3 GHz)

Polarization

L-band (HH, VV, HV, VH);
X-band (HH)

Methods of Measurement

SAR-Interferometry (Single path)
SAR-Polarimetry

Range Resolution

Resolution (Azimuth)
1,5 m (1 look), 4,0 m (4 looks)

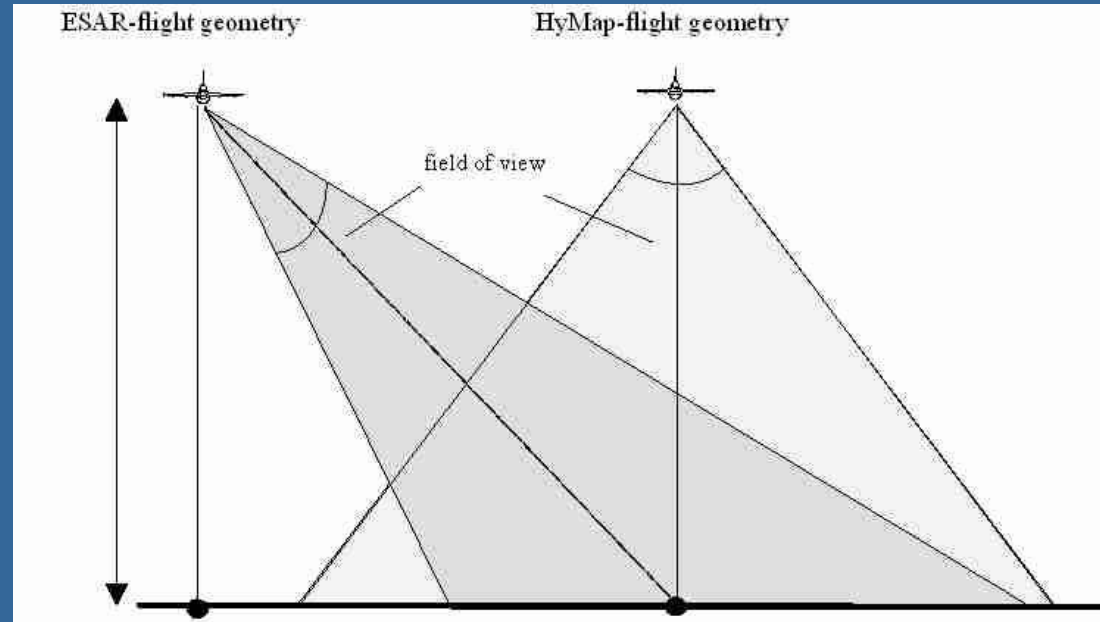


L-Band SAR-image of Oberpfaffenhofen

Many technical problems

- Localisation of corner reflectors;
- Single path interferometry produced bad interferogram (not yet operational);
- Some “read out” problems;
- Flew all the 3 X scenes again in the end of August 2005.

COMPARISON OF CHARACTERISTICS BETWEEN HyMAP AND E-SAR SENSORS



Parameter	Hyperspectral	SAR
Frequency	120 THz - 750 THz	1 GHz – 10GHz
Wavelength	0,4 μm – 2,5 μm	0,03 m - 0,3 m
angle of incidence	vertical	27° - 65°
Daytime/Nighttime	only usable during daytime	Daytime and nighttime
Weather dependence	not usable in bad weather	nearly independent of weather
Identification of materials	possible	impossible
Detection of surface condition (roughness)	impossible	possible

IMAGE PROCESSING METHODOLOGIES

Hyperspectral

Pre-processing (Radiometrical, atmospheric, geometrical, polishing and gain & offset corrections);

Data and noise reduction – MNF / PCA / LR;

Object detection based on logistic regression;

Classification based on LR / using the Matched Filtering (MF) / Mixture Tuned Matched Filtering (MTMF) algorithms;

Post-classification – Majority/Minority analysis.

SAR

Pre-processing (Speckle reduction using multi-looking and Gamma filtering);

Texture filtering (mean, homogeneity, dissimilarity, entropy, second moment & skewness);

Detection of dominant points;

Detection of man-made structure using Pauli-decomposition;

Classification – Maximum Likelihood

Fusion

Pixel based fusion (low-level fusion) of SAR multi-polarisation;

Pixel based fusion (low-level fusion) of SAR multi-channels (X, L);

Decision based fusion (high level fusion) of hyperspectral and SAR classification.

HYPERSPPECTRAL - OBJECT DETECTION

Based on Logistic Regression (LR)

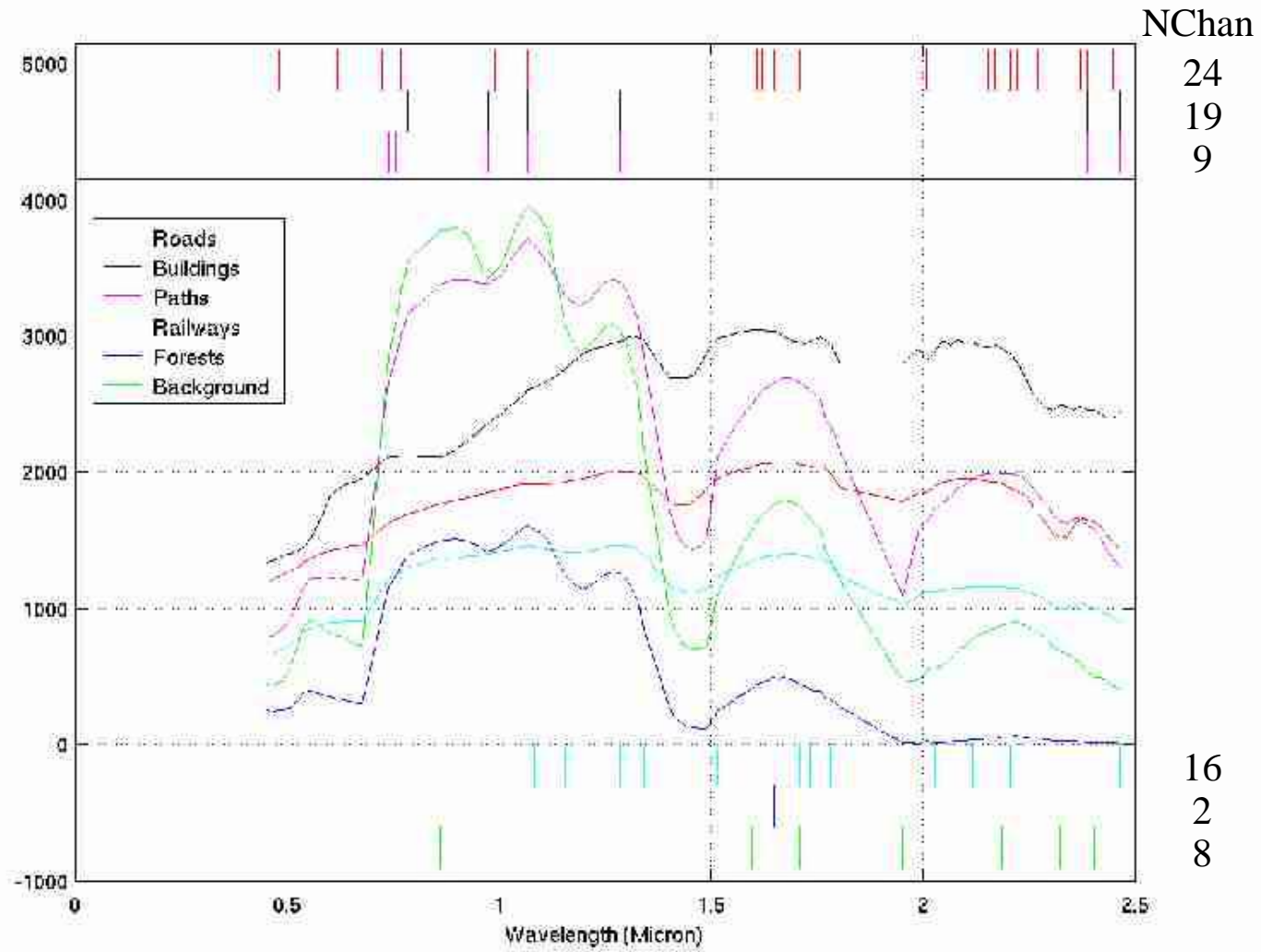
Logistic Regression

Finds an optimal combination of channels for detecting a given class, based on the learning set:

$$p_{x,y} \left(\text{TgtClass} \mid \vec{C} \right) = \frac{\exp \left[\beta_0 + \sum_{i=1}^N C_i(x, y) \beta_i \right]}{1 + \exp \left[\beta_0 + \sum_{i=1}^N C_i(x, y) \beta_i \right]}$$

Implicit channel selection by using step-wise optimisation method for finding β_i s.

Channel Selection by Logistic Regression



Results of the detector based on Logistic Regression

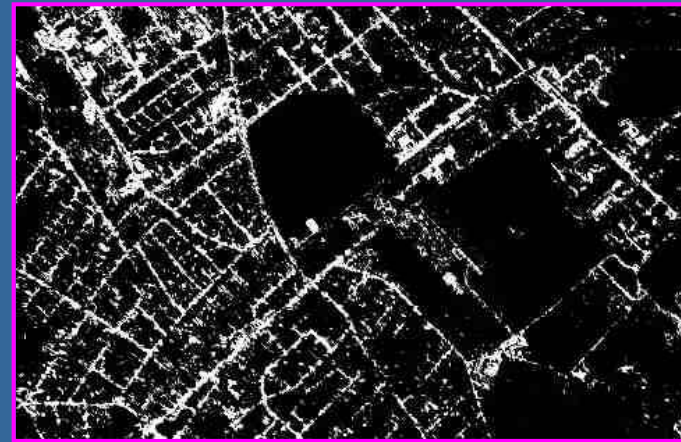
BruHyp Workshop, 7 October 2005, Bruges, Belgium



HyMAP image of Gilching, Germany
(R - 14, G - 9, B - 5)



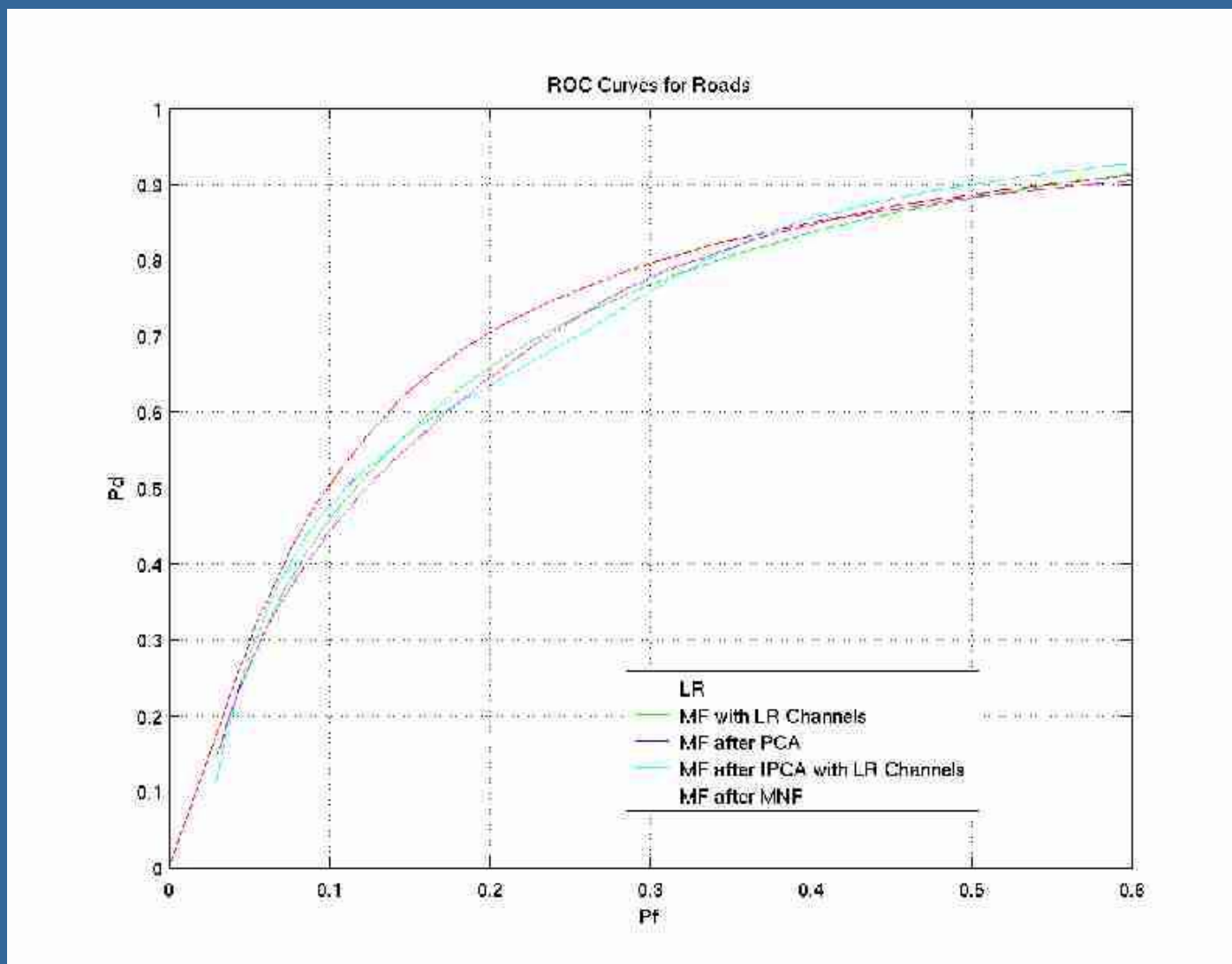
Buildings detection based on LR



Roads detection based on LR

Evaluation of channel selection and class detection

BruHyp Workshop, 7 October 2005, Bruges, Belgium



Classification based on Logistic Regression

BruHyp Workshop, 7 October 2005, Bruges, Belgium



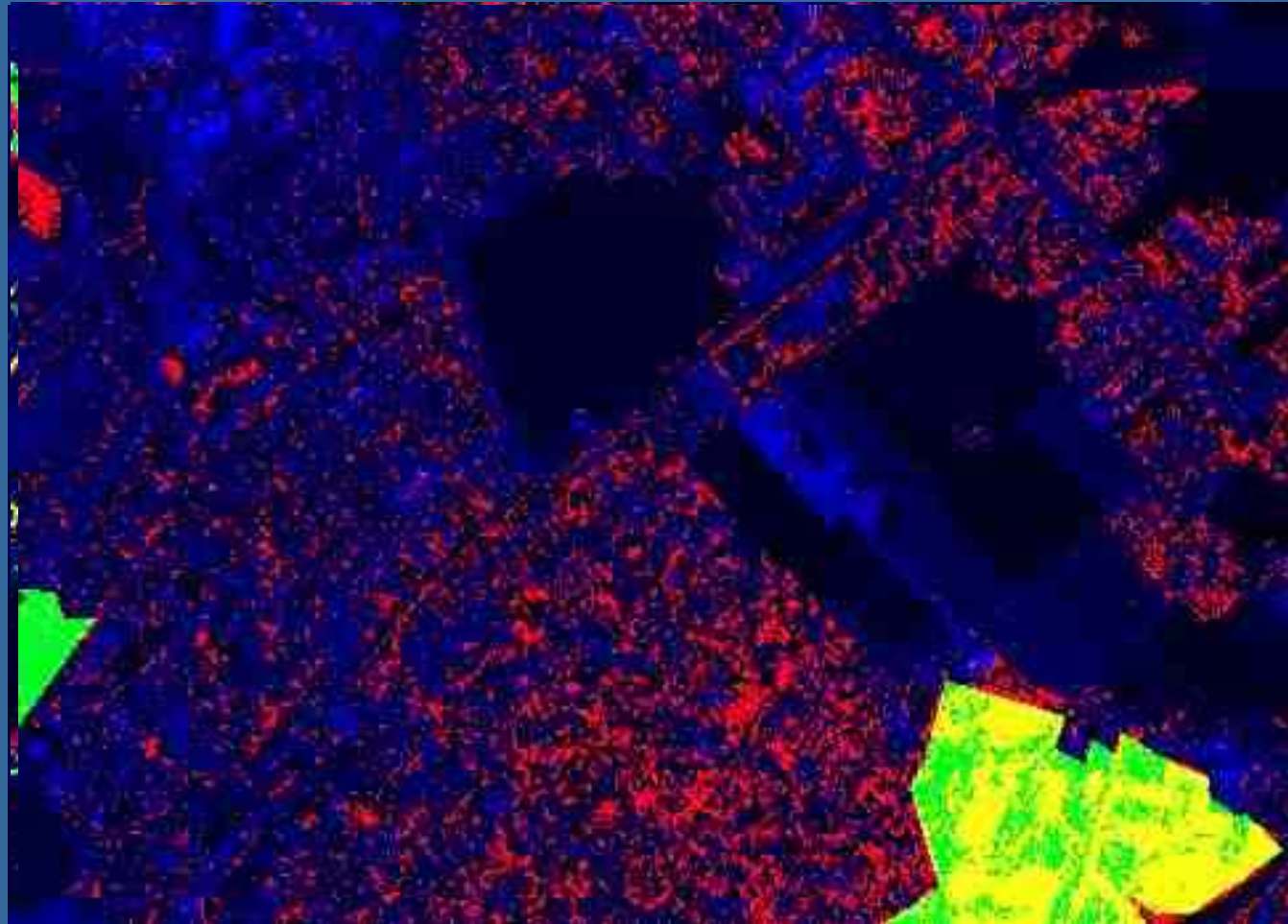
Classification based on LR

- Buildings
- Roads
- Paths
- Railways
- Background



Cadastral image

Evaluation of LR classification per Class



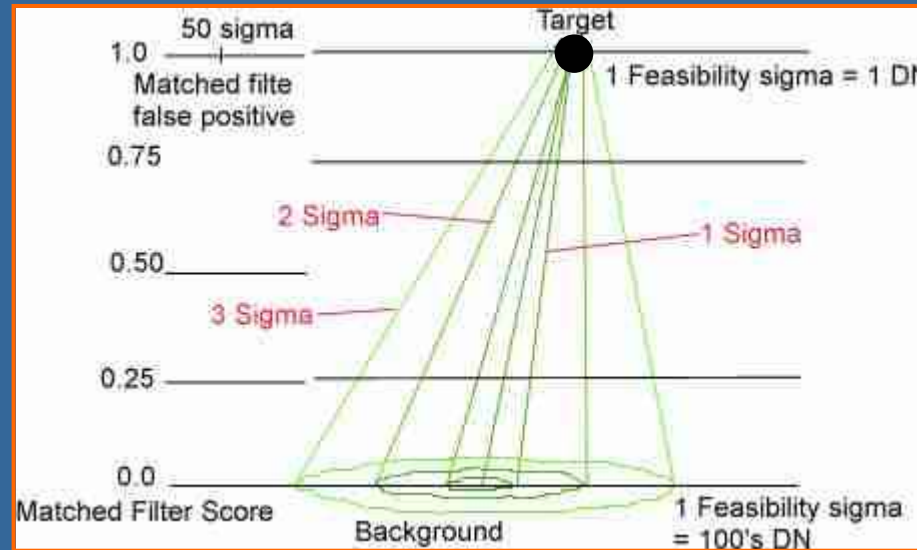
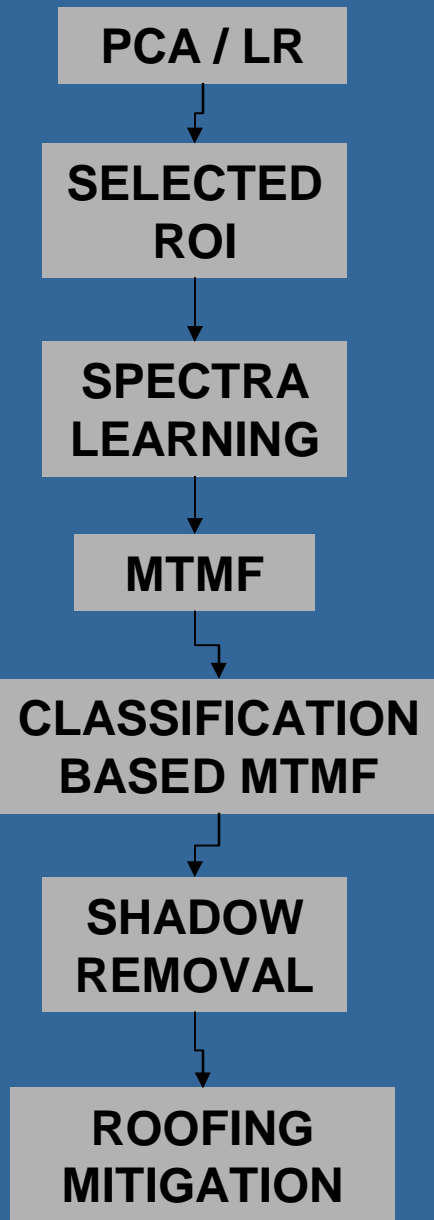
Forests

- Correct Detection
- Undetected
- False Alarm

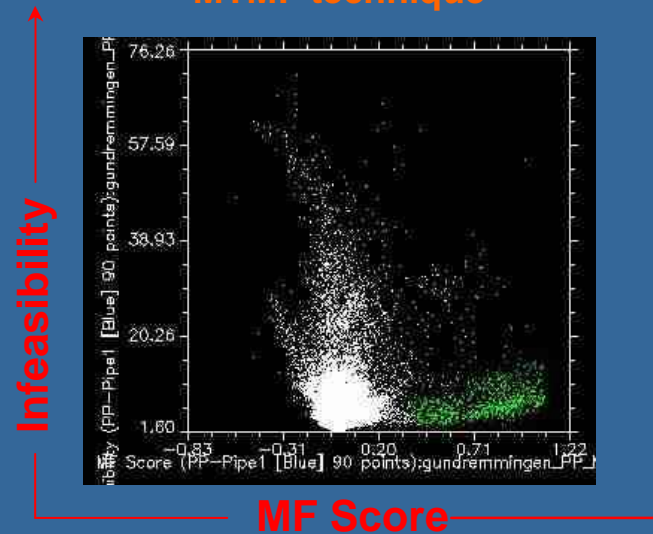
Detection Result Ground Truth One channel of image



HYPERSPPECTRAL – DISCRMINATION OF ROOF MATERIALS



MTMF technique



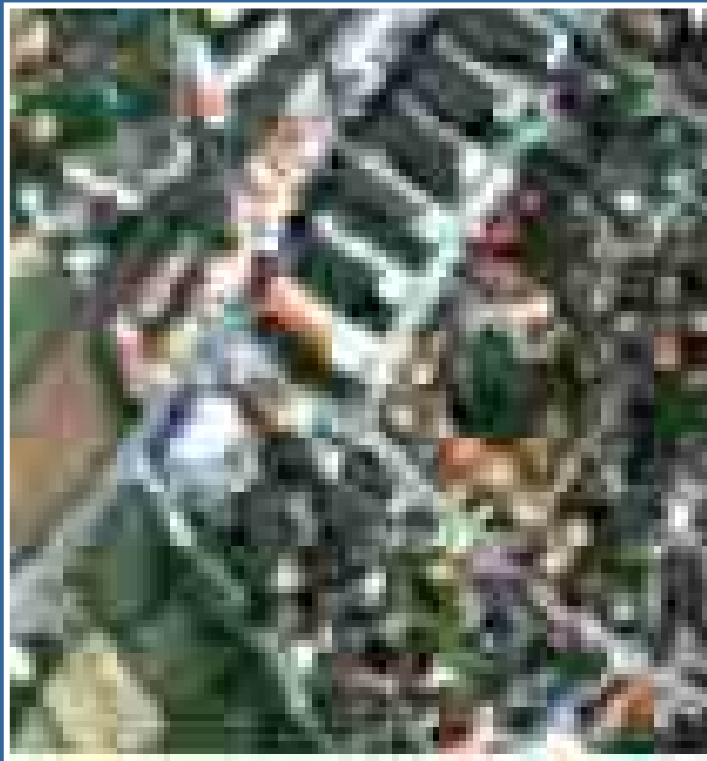


HyMAP image of Gilching, Germany
(R - 14, G - 9, B - 5)



 Tile - Clay (1)	 Shingles - fiberglass (1)
 Tile - Clay (2)	 Shingles - fiberglass (2)
 Tile - Concrete	 Conglomerate/asphalt
 Road asphalt	

MTMF classification of roofing materials (zoom-inn)



HyMAP image of Gilching, Germany
(R - 14, G - 9, B - 5)



 Tile - Clay (1)	 Shingles - fiberglass (1)
 Tile - Clay (2)	 Shingles - fiberglass (2)
 Tile - Concrete	 Conglomerate/asphalt
 Road asphalt	

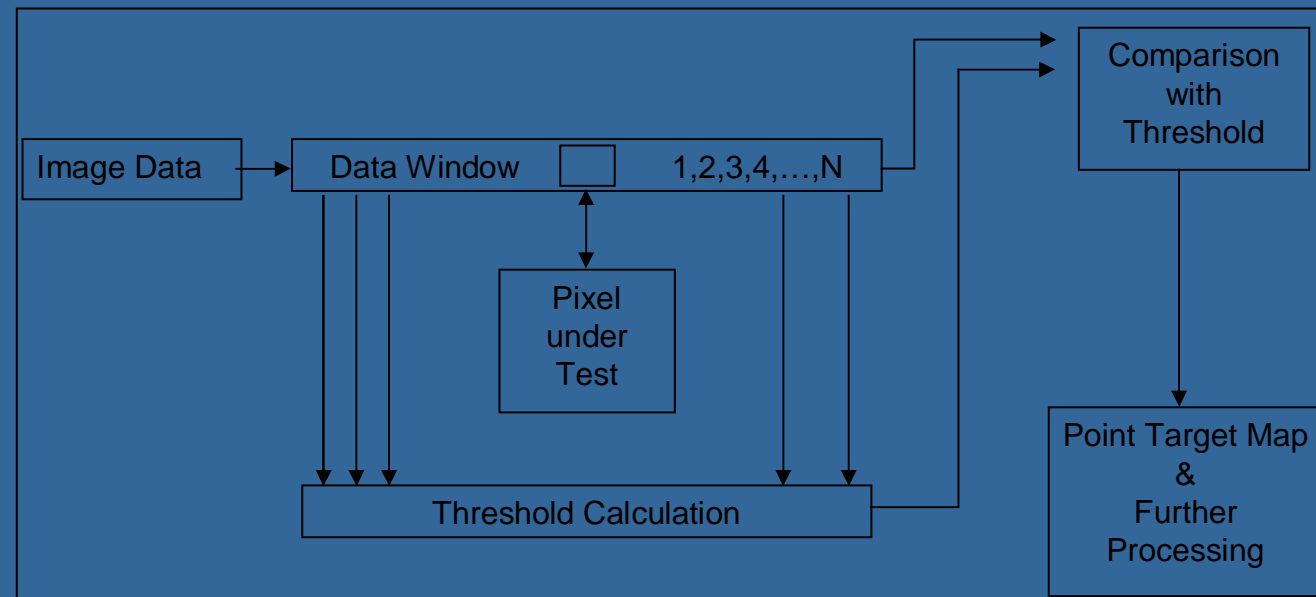
SAR - DETECTION OF DOMINANT SCATTER POINTS

BruiHyp Workshop, 7 October 2005, Bruges, Belgium



E-SAR / X image of Oberpfaffenhofen

Method for the detection of dominant scatter points



Detection of dominant scatter points - results



Point scatters on the E-SAR / X image of Oberpfaffenhofen

SAR – CLASSIFICATION OF MAN MADE STRUCTURE

Polarisation

Conventional SAR operate with a fixed single-polarization antenna for transmission and reception of radio frequency signals.

In this way only a single scattering coefficient is measured for a specific combination of transmitted and received polarization, which is proportional to the received backscattered power at a particular combination of linear polarization (HH, HV, VH or VV).

For a SAR system that coherently transmits and receives both signals from an an orthogonally polarized antenna pair, the scattering process can be modelled as a linear transformation described by a matrix $[S]$;

$$[S] = \begin{bmatrix} S_{hh} & S_{vh} \\ S_{hv} & S_{vv} \end{bmatrix} \quad (1)$$

Instead of the matrix notation, one may use a four element complex vector \vec{k}

$$[S] = \begin{bmatrix} S_{hh} & S_{vh} \\ S_{hv} & S_{vv} \end{bmatrix} \rightarrow \vec{k} = \frac{1}{2} \text{Trace}([S]\Psi) = [k_0, k_1, k_2, k_3]^T \quad (2)$$

where $\text{Trace}([S])$ is the sum of the diagonal element of $[S]$ and Ψ is a complete set of 2×2 complex basis matrices.

The Pauli basis (formed by the pauli spin matrices)

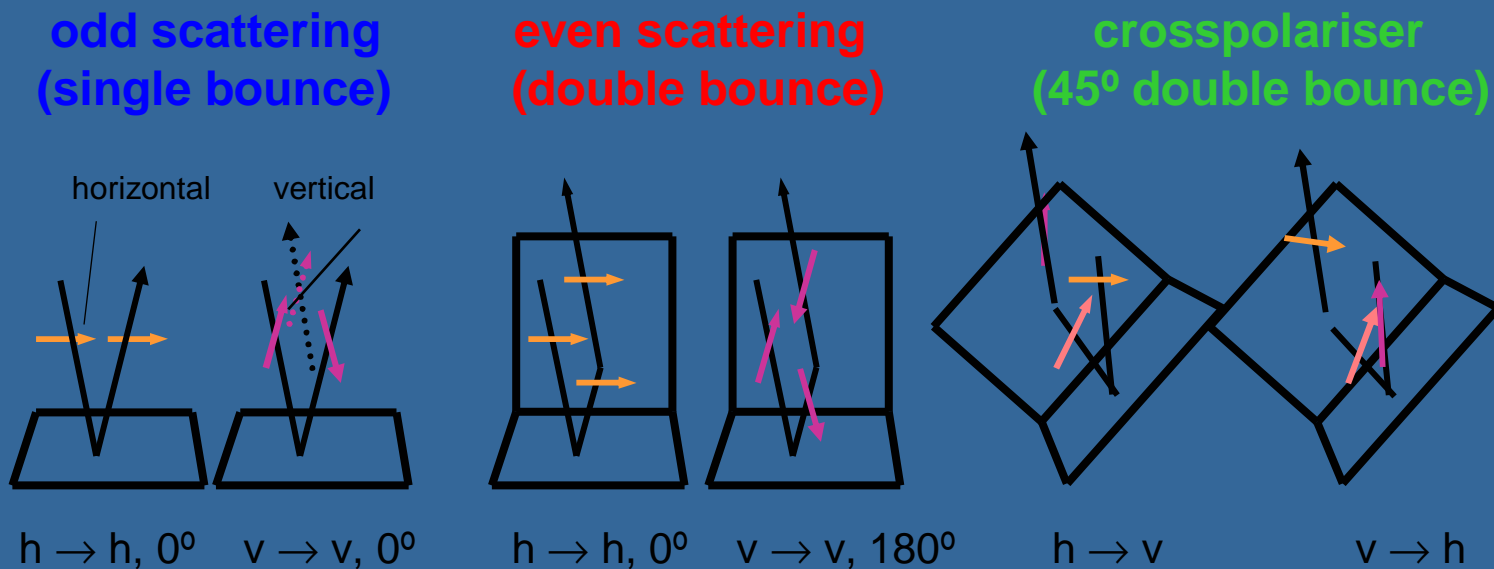
$$\Psi_\rho = \left\{ \sqrt{2} \begin{bmatrix} 1 & 0 \\ 0 & 1 \end{bmatrix}, \sqrt{2} \begin{bmatrix} 1 & 0 \\ 0 & -1 \end{bmatrix}, \sqrt{2} \begin{bmatrix} 0 & 1 \\ 1 & 0 \end{bmatrix}, \sqrt{2} \begin{bmatrix} 0 & -i \\ i & 0 \end{bmatrix} \right\} \quad (3)$$

The corresponding vector \vec{k}_ρ is then

$$\vec{k}_\rho = \frac{1}{\sqrt{2}} [S_{hh} + S_{vv}, S_{hh} - S_{vv}, S_{hv} + S_{vh}, i(S_{vh} - S_{hv})] \quad (4)$$

Pauli decomposition in SAR

The Pauli decomposition is calculated from the original single look complex radar data and provides information about three independent scatter mechanisms in three channels:



$$R G B - HH, VV, (HV+VH)/2$$

Pauli decomposition channels R G B - HH , VV , $(HV+VH)/2$



Pauli decomposition of E-SAR / L-Band SAR image (R : even scattering, G : crosspolariser, B : odd scattering)

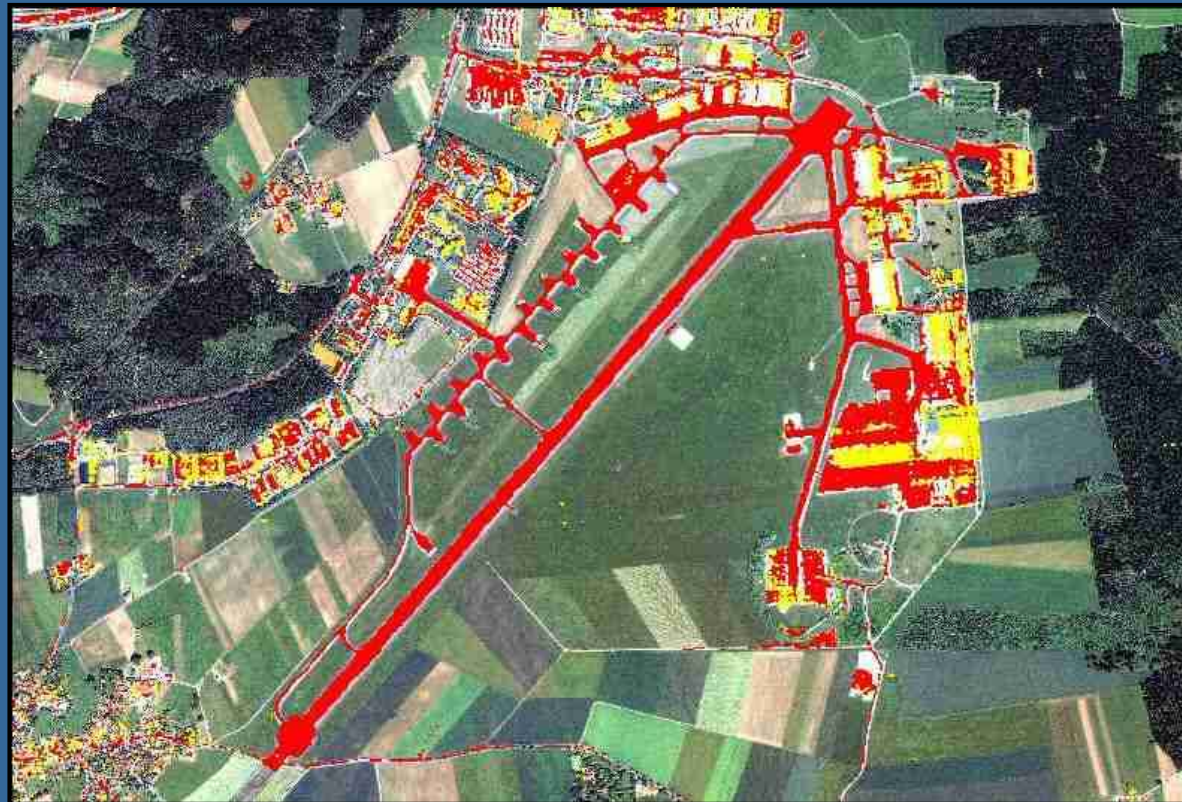


Maximum likelihood classification of L-Band E-SAR data based on Pauli decomposition

- Forest
- Roads and runway
- Buildings
- Grassland

COMBINATION OF SAR AND HYPERSPPECTRAL DATA

Pixel based fusion demands sub-pixel accuracy;
Decision (context) based fusion demands pixel accuracy.



- Roads
- Buildings

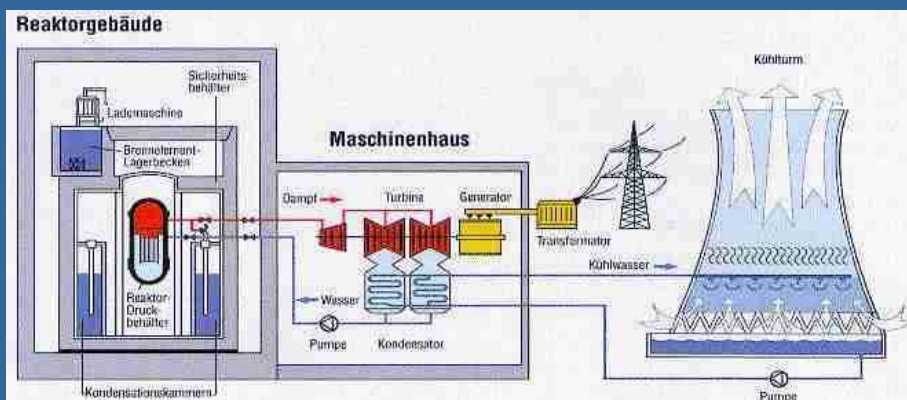
Combination of SAR and Hyperspectral classification results superimposed on IKONOS high resolution image

GUNDRREMINGEN NUCLEAR POWER PLANT

BruHyp Workshop, 7 October 2005, Bruges, Belgium



The first of three boiling-water nuclear reactors at Germany's Gundremmingen plant began operating in 1966 but was permanently shut down after being decommissioned in 1983.



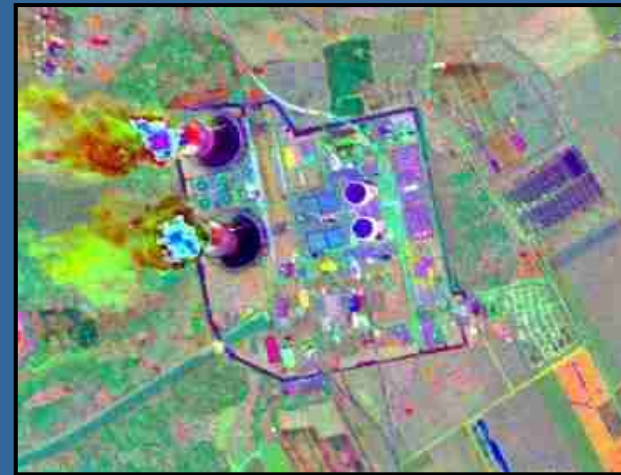
Additional cooling systems were installed for the remaining two operational reactors at the plant in 1995.

POWER PLANT - HYPERSPECTRAL

BruHyp Workshop, 7 October 2005, Bruges, Belgium



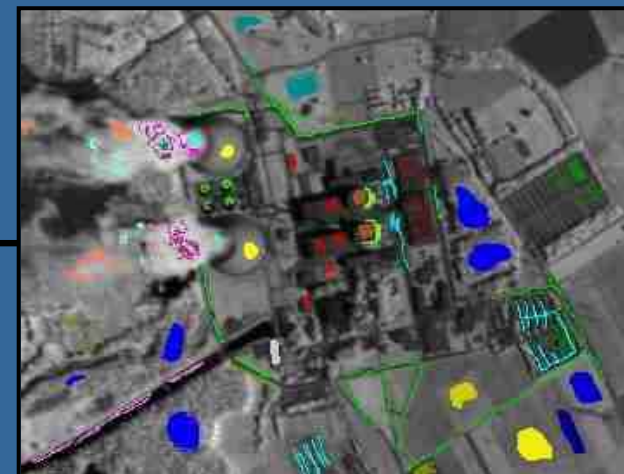
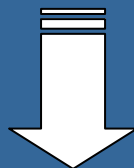
HyMap RGB (B14, B9, B5)



MNF component (C4, C3, C2)



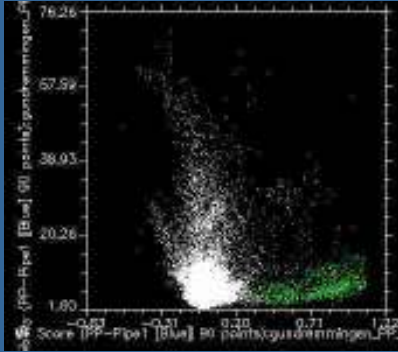
SPECTRA LEARNING (18)



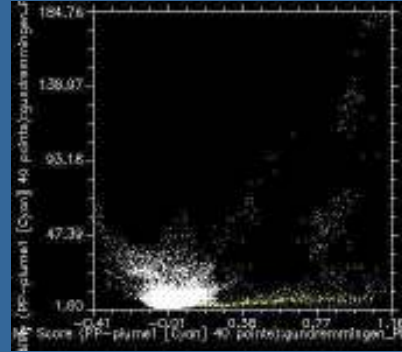
Selected ROI on MNF (26)



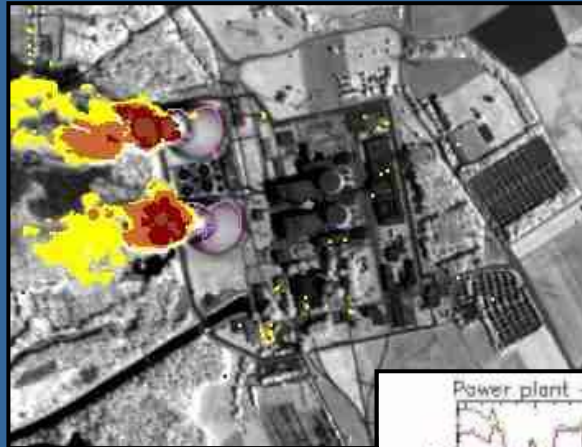
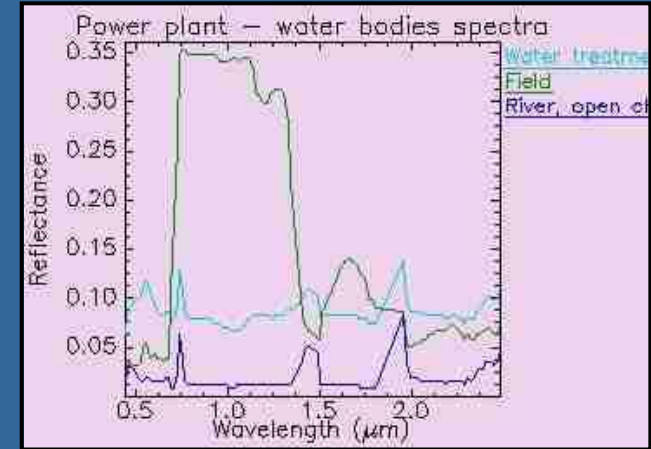
Matched Filtering (MF)



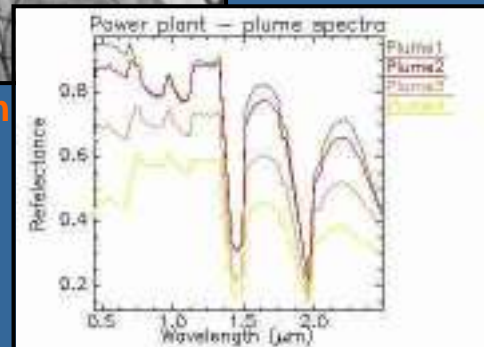
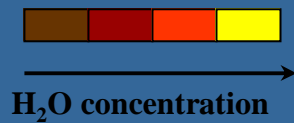
Cooling tower



Plume



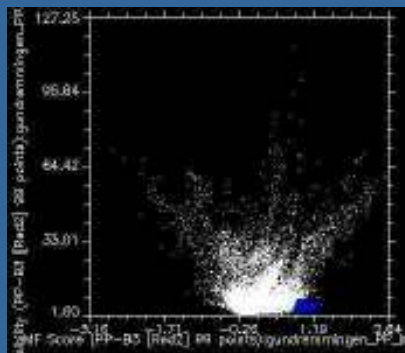
Plume classification using MF



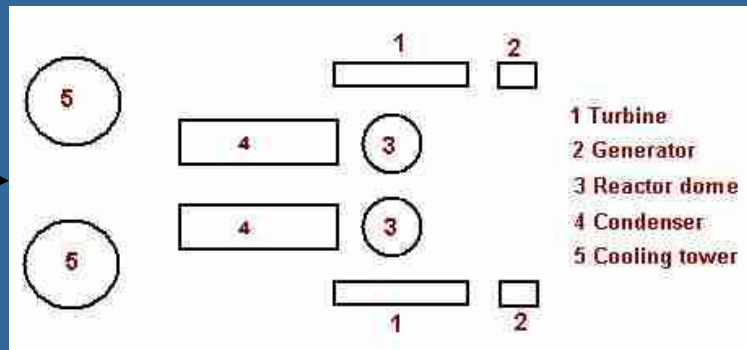
Water classification using MF

POWER PLANT Structures

BruHyp Workshop, 7 October 2005, Bruges, Belgium



Dome structure



Power plant structures diagram based on the classification results



Power plant structures classification using MF

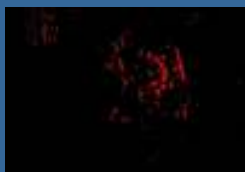


Power plant structures, roads and fences classification using MF

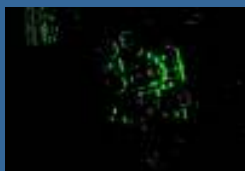
POWER PLANT – SAR/ X_{HH}

BruHyp Workshop, 7 October 2005, Bruges, Belgium

TEXTURE FILTERS



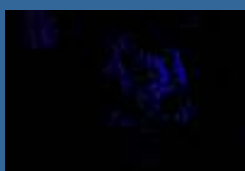
Dissimilarity



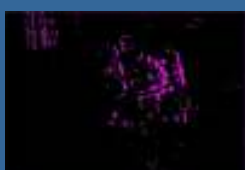
Entropy



Mean



Homogeneity



Second moment



Power plant – ESAR x band



Power plant – Synthetic colors



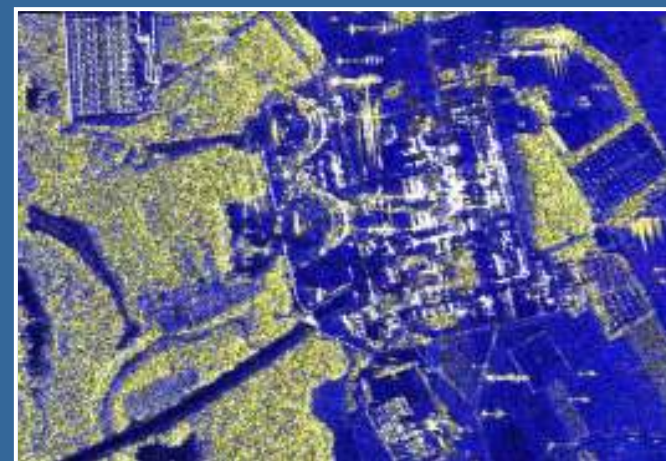
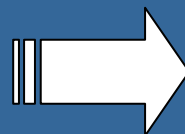
Power plant structure – Fusion of 5 different texture filters

POWER PLANT – SAR/L_{full} polarisation

BruHyp Workshop, 7 October 2005, Bruges, Belgium



Power plant – ESAR / L full polarisation



Pauli decomposition – R (HH)
G (VV) B ((HV + VH)/2)



Texture Filter (skewnes)

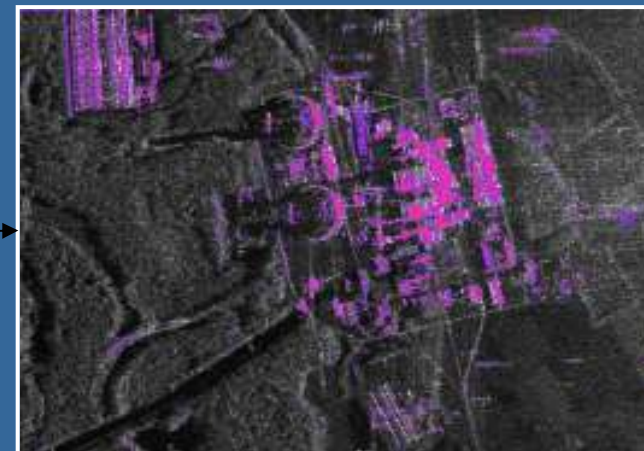
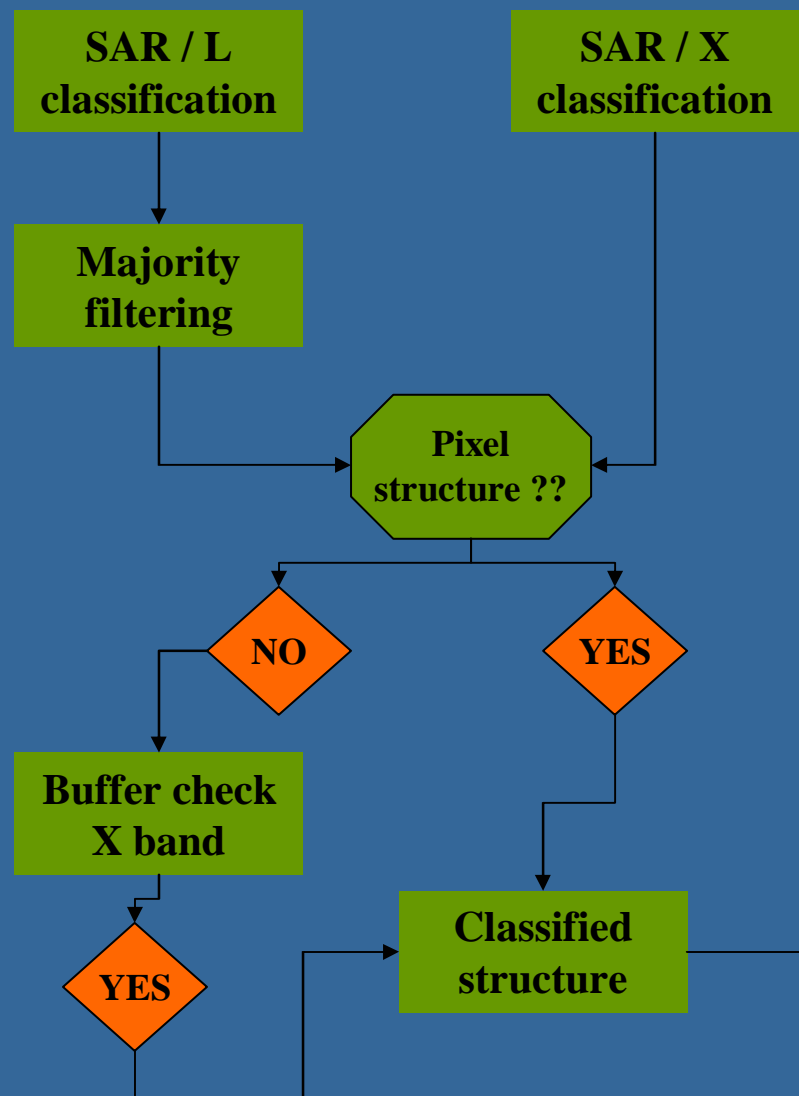


Texture filter (skewnes) results over the pauli decomposition

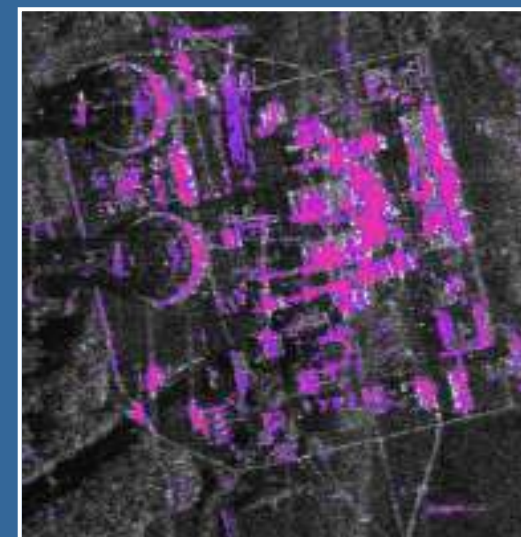
POWER PLANT – SAR

Pixel based fusion - X and L bands + polarisations

BruHyp Workshop, 7 October 2005, Bruges, Belgium



Fusion results X (magenta) + L (purple) bands



Conclusion and future research

Logistic regression used for man made object detection, channel selection and classification

Is fast and accurate technique for robust classification of man made materials;

Is a good technique for hyperspectral data reduction;

An extensive ground truth data is no needed;

The robust classification made using LR produced better results than MF.

Future research

Physical explanation for selected channels;

Influence of pre-processing level.

For hyperspectral data it is possible to rely on a pixel-wise classifier for extraction of residences, roads, industrial buildings and building materials.

For SAR images a pixel-wise classifier can be used for large buildings or for identifying built-up areas. However it is not possible to detect individual houses in an urban environment using SAR, mainly due to the imaging geometry.

“Point scatterers” detected in SAR images are strongly correlated with man-made structures signals.

A classifier based on polarimetric decomposition methods is useful for detection of large buildings and roads in SAR. However, a specific detector for linear feature is more effective for smaller roads and buildings.

Combining SAR multi-channel information produces better detection and classification of man-made structures than single channel data.

Generally, we have found that data fusion of SAR- and hyperspectral data give complementary information regarding the urban scene and are useful for road detection. However, data fusion of E-SAR and hyperspectral was not sufficient for building detection due to difference imaging geometry.

Refined methods have to be developed and applied for future improvements.